Monte Carlo entropic sampling for the study of metastable states and relaxation paths

Isidor Shteto, Jorge Linares, and François Varret
Laboratoire de Magnétisme et d'Optique, CNRS, Université de Versailles, St. Quentin en Yvelines, 45 Avenue des Etats Unis, F78035 Versailles Cedex, France
(Received 24 June 1997)

We present a continuous extension of the recent Monte Carlo entropic method for sampling a density of states restricted in dimensionless macroscopic parameters. The method performs a random walk through a two-dimensional macrostate space and provides complete information in the form of continuous functions of the system's coupling constants. For the example of an Ising system, we project relaxation paths from Monte Carlo Metropolis dynamic over the two-dimensional state space and compare them with a ''most probable path'' associated with the equilibrium distribution, derived from the density of states. We observe a close agreement between them in the stochastic regime, i.e., before the system escapes from the metastable state. We establish a Markovian macroscopic dynamic over the two macroscopic parameters and we discuss it with respect to the Metropolis microscopic dynamic. [S1063-651X(97)01511-0]

PACS number(s): 64.60.My, 05.50.+q, 05.70.Ln, 64.60.Qb

I. INTRODUCTION

It is very interesting, for the study of the equilibrium and nonequilibrium properties of a system, to access its fluctuations. It is now well established that equilibrium fluctuations play an important role in nonequilibrium thermodynamics. They are central to an understanding of nucleation phenomena and metastable states related to them. Metastable states are very common in nature, and a very large class of apparently stable states are actually metastable but very long lived. Many crystallographic phases associated with structural phase transitions (e.g., diamond) are metastable state with astronomical lifetimes. Experimentally these states are observed near first-order phase transitions in different contexts, e.g., parts of hysteresis loops associated with the magnetization reversal in a ferromagnet or with phase separations in alloys, supercooled vapor, and superheated liquid, switching behavior in ferroelectric films or bistable molecular systems [1–5].

The question of the existence and properties of metastable states still remains a challenge to the theoretical physicist. Metastability is obviously, in almost all real systems, a kinetic phenomenon, except for some infinitely long-lived metastable phases in systems with weak long-range interactions. It was demonstrated in the infinite-system formalism that one-phase systems with short-ranged interactions cannot support infinite long-lived metastable states [6–9]. If the interactions are short ranged only a finite-energy fluctuation (sometimes very large) is needed in order for the system to escape from the metastable phase: nucleation barriers are finite even in the thermodynamic limit. However, the lifetimes may be very long even in a short-ranged interaction system [10,11,9,12,13], and as long as the system remains ''truly metastable'' (i.e., does not decay), it is possible to perform measurements of thermodynamic quantities such as specific heat or susceptibility. These ''equilibrium'' properties lead to an interesting fundamental challenge aimed at describing metastable states from a statistical physics point of view. Statistical mechanics has a well-defined ''canonical'' formalism for obtaining the equilibrium properties of macroscopic matter, and also, to a lesser extent, the nonequilibrium properties of systems close to equilibrium. There is, however, no such formalism for metastability and nucleation in finite systems, only a collection of *ad hoc* methods, most of them approximate, for particular problems. The only rigorous treatment of Penrose and Lebovitz [14] holds for systems with weak long-ranged interactions (liquid-gas transition), where the metastable phase is formally described in terms of restricted equilibrium ensembles excluding microstates which dominate at equilibrium (for a detailed discussion about the relevance of different treatments, see Ref. [15]). For short-ranged models, there is no unique way to construct such restricted ensembles, i.e., to define a metastable configuration space. Nevertheless, the arbitrary nature of the restriction has no real practical incidence on the deduced properties of the metastable state, as long as the latter are very long lived [10,15]. Hence, for short-ranged models the above treatment is only as a conjecture, suggesting that a system remaining in a metastable state samples the associated configurations according to their relative weight in the partition function.

Different efforts have been made to demonstrate the relevance of equilibrium properties in describing the relaxation of a metastable state. The relation between nucleation barriers and the shape of the restricted free energy $F(m)$ in finite systems have been studied by Schulman [16] and also by Binder and co-workers [17–19]. Nucleation rates with different dynamics—cluster Swendsen-Wang dynamics or local Metropolis-like dynamics (see Refs. [20,21], and refs. included)—pointed out that metastable properties which are functions of equilibrium or *quasiequilibrium* bulk quantities are the same in both dynamics. Recently, a detailed study on the relaxation of metastable phases in an Ising ferromagnet [22] showed that the restricted bulk free energy $F(m)$ provides the essential characteristic behaviors of the latter when used to construct a local macroscopic mean-field-like dynamic.

In this paper, we mainly focus on the possibility of describing the metastable phase fluctuations by equilibrium distributions (ED's). The above considerations suggest that any dynamic which obeys the detailed balance statement, in addition to giving the correct equilibrium properties, would also give the correct *quasiequilibrium* properties for the metastable state. Therefore, we can expect that the metastable phase's microscopic configuration space will be explored according to ED's. If we project the latter over some macroscopic variables, say total magnetization m and energy E of the well-known Ising model, it turns out that the two-dimensional macroscopic configuration space resulting from this projection would be explored, obeying the corresponding macroscopic distribution $P(m,E)$.

The first advantage of a two-variable macroscopic state is the possibility of vizualizing relaxation paths. We analyze the possibility that not only small fluctuations but also large fluctuations, contributing to the escape from the metastable phase, may be described by ED's. Typically, we think that the comparison between the Metropolis dynamic's two-dimensional relaxation paths from the metastable phase to the stable phase, and the equilibrium distribution surface of that system may be very informative. Hence, we investigate how long it is possible to have an information on the long-range equilibrium fluctuations in a reduced space, only by examining the whole spectrum of the projected ED's in that space. Then, a mean-field-like Markovian macroscopic dynamics may be constructed as an approximation of the exact projection of Markovian microscopic dynamics—Metropolis, Glauber, heat bath—over the macroscopic states $\{m,E\}$, as is done in Ref. [22] for a one-dimensional space described by $F(m)$. A quantitative comparative study of the approximation's quality for the one-and two-variable mean-field-like dynamics is beyond the scope of the present study. We just aim to point out the possible correlations between the quality of the macroscopic dynamic approximation and the properties of the ED surface.

The knowledge of the probability surface implies a complete exploration of the reduced state space. This may be done exactly for small systems (up to 6×6), just by enumerating exhaustively all microscopic configurations; for larger ones, recent new Monte Carlo sampling methods have been very successful. We use the entropic sampling method [23] that we adapted for sampling and storing a two-dimensional density of states $D(E,m)$. This is reported in Sec. II, where we describe, for the example of an Ising-like model, how to obtain a density of states which is independent of the Hamiltonian's parameters. Then we show how relaxation paths may be predicted from ED's. (Sec. III), and in Sec. IV we briefly define and apply a two-variable macroscopic dynamic before discussing the results in the perspective of multivariable macroscopic dynamics as approximations of the microscopic dynamic.

II. EQUILIBRIUM DISTRIBUTIONS BY MONTE CARLO CALCULATIONS

It is clear that the Monte Carlo Metropolis algorithm (see, e.g., Ref. [24]) is not suited to access the whole spectrum distribution of observable features of the system. It only explores the most probable configurations, implying short-range fluctuations. Several variants of the Metropolis algorithm have been proposed [25–28] to overcome the problem, basically consisting of exploring several areas of the state space, by using several sets of coupling constants (temperature, interactions, energy gaps, etc.). They face serious difficulties for connecting the separate pieces of information, mostly in the case of high-energy barriers. Recently, Lee [23] introduced a biased Monte Carlo method, the so-called ''entropic sampling method,'' which was shown to be equivalent to the previous Berg's Multicanonical method [29,30,22]. The Lee entropic sampling actually samples the density of states, and since all areas of the state space are visited, the necessary information for all temperatures is obtained in a single sampling procedure.

In this paper we use the entropic sampling method for storing a two-variable density of states. This is done for the simple example of an Ising-like system under a field, with unique and constant nearest-neighbor interactions. The whole spectrum of the statistical distribution is derived as a continuous function of the model parameters.

A. Multidimensional densities of states for complete equilibrium descriptions

Starting from the well-known Hamiltonian, with $\sigma_i=\pm1$ eigenvalues

$$\hat{\mathcal{H}}=-h\sum_i \hat{\sigma}_i-J\sum_{\langle i,j\rangle}\hat{\sigma}_i\hat{\sigma}_j, \tag{1}$$

the total energy is expressed in terms of dimensionless quantities, proportional to $m=\Sigma\sigma_i$ and the nearest-neighbor correlation $s=\Sigma\sigma_i\sigma_j$:

$$E=-hm-Js. \tag{2}$$

The canonical partition function is expressed in terms of the dimensionless quantities,

$$Z_\beta=\sum_{m,s} N(m,s)\exp[-\beta(-hm-Js)], \tag{3}$$

with $\beta=1/k_BT$, and where $N(m,s)$ is the number of configurations for a given set of values, and $\{m,s\}$ is actually the degeneracy of the macrostate $\{m,s\}$. $N(m,s)$ is of central interest here, and much macroscopic thermodynamical information can be derived from it. In a continuous approximation, it should be substituted by the restricted density of states $D(m,s)$; for convenience, $N(m,s)$ here will be termed the density of states. The degeneracy of the energy level E is

$$N(E)=\sum_{m,s;E} N(m,s), \tag{4}$$

where the sum is carried on all $\{m,s\}$ macrostates of given energy E. The corresponding equilibrium probabilities are

$$P_\beta(m,s)=N(m,s)\exp(-\beta(-hm-Js)/Z_\beta. \tag{5}$$

The restricted partition function $Z_\beta(m)$ and the resulting probabilities $P(m)$ are then derived:

$$Z_\beta(m)=\sum_s N(m,s)\exp[-\beta(-hm-Js)], \tag{6}$$

$$P_\beta(m)=Z_\beta(m)/Z_\beta. \tag{7}$$

In addition, all macroscopic equilibrium quantities, e.g., specific heat or susceptibility, can be derived from $N(m,s)$ analytically for any set of parameter values and any temperature. The method is, in principle, easily extended to more complicated Hamiltonians: the basic idea is that each energy term in the Hamiltonian is represented by a macroscopic (dimensionless) variable; the state space is constructed along these macroscopic variables. Also, in the case of large systems, the state space can be gridded, and the method follows in proper terms of the density of states. An attractive feature of the method is that the sampling is performed only once, for a system of given size and interaction topology, even for various degeneracies attributed to the spin states, or when switching from ferromagnetic to antiferromagnetic interactions.

B. Entropic sampling for bidimensional density of states

In this section we describe how the biased Monte Carlo sampling method, called entropic sampling [23], is used to calculate the density of states, i.e. the microcanonical entropy, and we give some details on how it runs and converges.

The entropic sampling method [23] relies on the idea that a Monte Carlo (MC) procedure yields any desired distribution **P**, provided that the same distribution is introduced as a bias in the detailed balance equation. Such a property derives from the properties of the Markov chains, irrespective of the actual physical process. To achieve a complete exploration of the state space, a biased method has to favor configurations belonging to weakly degenerate macrostates (small density of states), and to dampen those belonging to the highly degenerate macrostates (large density of states); the latter are those sampled by a simple sampling or by an importance sampling (the Metropolis algorithm) at high temperatures. The biasing probability, which is suited for an uniform exploration of the state space, merely is the inverse of the restricted density of states. Since the latter is *a priori* unknown, a good starting approximation, as suggested in Ref. [23], is the density of states of a similar system of smaller size, previously determined in some way, and then scaled for the larger size system. The process can be run iteratively, and we term $N_i(m,s)$ the density of states obtained after iteration i. Then, using $N_i(m,s)$ as a bias, a MC sampling is run; it is termed a ''Monte Carlo stage,'' and yields a histogram of the frequency of the macrostates: $H_i(m,s)$. Once corrected for the bias, the resulting restricted density of states is obtained as

$$N_{i+1}(m,s)\sim N_i(m,s).H_i(m,s). \tag{8}$$

It must be pointed out that all involved quantities are dimensionless, e.g., there is no temperature (as in Ref. [23]) at this stage of the method. Equation (8) may yield at once, i.e. through a single MC stage, the correct result, for a great number of MC sweeps, even if the initial density is far from correct. In practice, the method is better used iteratively, with, according to Eq. (8), the flat character of the histogram $H(m,s)$ as a convenient convergence criterion.

As for the numerical limitations of the method, it is clear that they mainly lie in the random procedure. We observed that the relative scatter of the histogram after a given MC stage depends both on the quality of the initial density distribution and on the number of MC sweeps per macrostate for a stage; the total number of macrostates is proportional to N^p, with N the number of spins, and p the number of dimensionless parameters. An optimum strategy consists of starting with short stages and then increasing the length of the next stage if either the quality of the histograms (the mean ''flatness'') is not improved or the number of visited macrostates has decreased. As an example, for the 32×32 system, we started with 10^4 MC sweeps, and finished the calculation with the three final MC stages from 8 to 15×10^7 MC stages; at the final stage the resulting histograms presented a mean standard deviation of 2%.

It is clear that calculations for larger systems are no longer reasonable if one continues to project configurations over the discrete set of the $\{s,m\}$ values, because of the N^2 law for the number of macrostates. Using an IBM RS/6000 560 computer with 100 megaflops, the reasonable practical limit seems to be around 1000 spins for the present example, where we want to obtain a two-parameter information; the maximum size of the planar system is then 32×32, giving 498 252 macrostates, reduced to 249 126 using $D(-m,s)=D(m,s)$ symmetry. For comparison, the multicanonical ensemble Berg's method can treat up to 64×64, but has to be repeated for each temperature, as in Ref. [22]. For larger sizes, one could proceed in terms of a continuous density of states with a grid state space in order to limit the number of macrostates to be sampled. However, the grid's intervals along the energy dimension must not be large compared to k_BT.

We illustrate the method with an 8×8 square planar Ising system. The initial density has been obtained via a Gray code on a 4×4 system. In Fig. 1 we show the random walk of the sampling algorithm; the iterative process included four MC stages, each made of 10^6 MC stages. In Fig. 2 we plot the average squared displacement, in the fourth MC stage, as a function of the number of MC stages, i.e., as a function of the elapsed time. It is concluded from both figures that the desired uniform exploration of the state space has been correctly achieved, as a random, diffusionlike, walk, through a converging iterative process. In Fig. 3 we present the histogram provided by the fourth MC stage. As desired, it is reasonably flat. As a check of the reliability of the method, we show in Fig. 4 the specific heat computed for several square planar systems of finite size ($L=8$ and 16, $h=0$), which compare quite well to the exact Onsager solution.

III. EQUILIBRIUM PROBABILITY SURFACE AND RELAXATION FROM METASTABLE STATES

We focus here on the properties of metastable states in ferromagnetic systems with short-range interactions, prepared in a total magnetization configuration opposite to the applied field. Again we use the nearest-neighbor Ising system. The metastable lifetime $\langle\tau\rangle$ in such systems has been extensively studied analytically and by Monte Carlo simula-

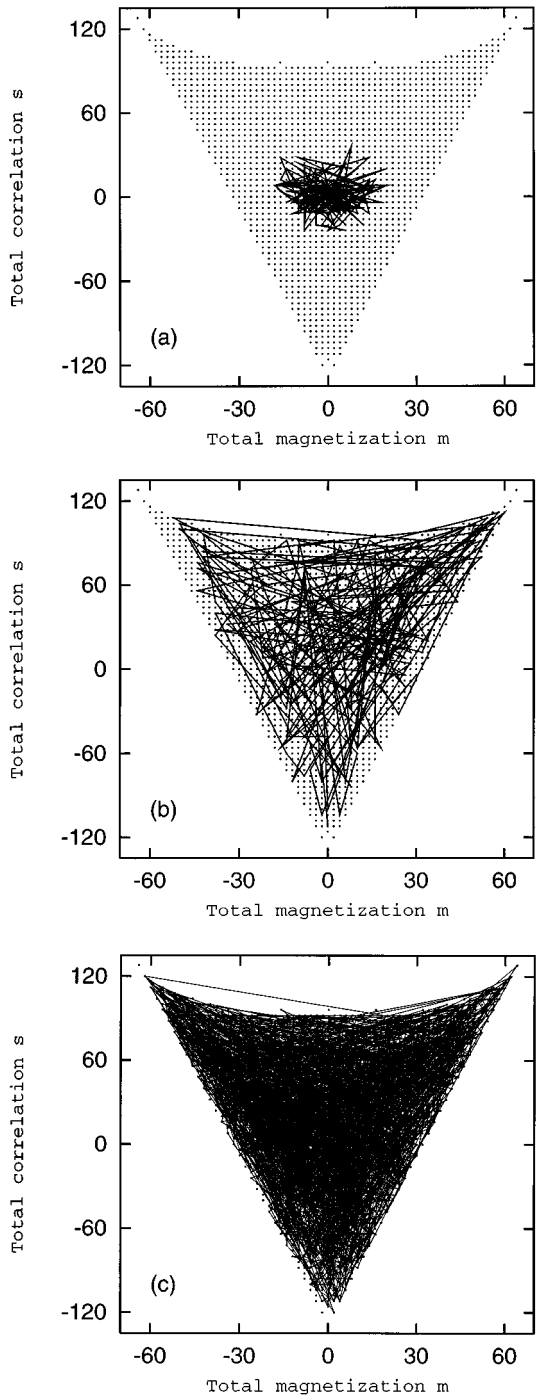

FIG. 1. Random walks in the (m,s) state space for an 8×8 lattice. The dots show the accessible states. The broken line represents the pathway, scanned every 5000 Monte Carlo steps per spin: (a) first Monte Carlo stage; (b) fourth Monte Carlo stage. Bottom (c): fourth Monte Carlo stage scanned every 500 Monte Carlo sweeps.

tions. Indeed, the field-theoretical droplet theory of Langer [31–33] was shown to be a valid approach by Monte Carlo simulations in local Metropolis or Glauber dynamics [20].

These results, and some earlier ones, on the field and system's size dependence of the metastable lifetime of the Ising model can be summarized through the following concepts. (i) Critical droplet: the relaxation of the metastable phase develops by nucleation and growth of droplets of the ''stable

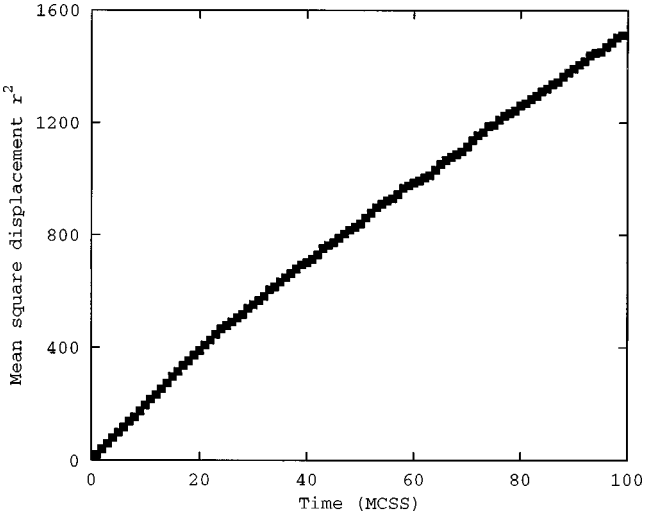

FIG. 2. Mean-square displacement $\overline{\delta r^2}$ [in units of the (m,s) cell parameter] as a function of time [in units of Monte Carlo steps per spin (MCSS)], in the (m,s) plane $(8\times8$ lattice).

phase'' (in which the magnetization is parallel to the applied field). Small droplets are continuously created and destroyed by thermal fluctuations. Below (above) a critical size, due to the balance between the bulk and the interface energies, the droplet has a high probability of vanishing (growing). The size of the critical droplet does not depend on the system's size; it follows the ratio interaction and/or field. Thus the decay properties clearly depend on the relative sizes of the system and the critical droplet. Large systems have a higher probability to possess nucleation centers and then the lifetime is inversely proportional to the number of sites. (ii) Dynamical spinodal point: when varying the field, at a given system's size, two important regions are distinguished; at small fields a single-droplet (SD) feature of nucleation is observed and at larger ones the nucleation is a multidroplet (MD) process. The crossover field between the two features was called the ''dynamical spinodal point'' (DSP) [34], and depends on temperature and system size. The decay process has qualitatively different behaviors in the two regions. In the SD region the average metastable lifetime $\langle\tau\rangle$ is very long but is inversely proportional to the system volume [12,20,31–36]; the decay approximately follows a Poisson

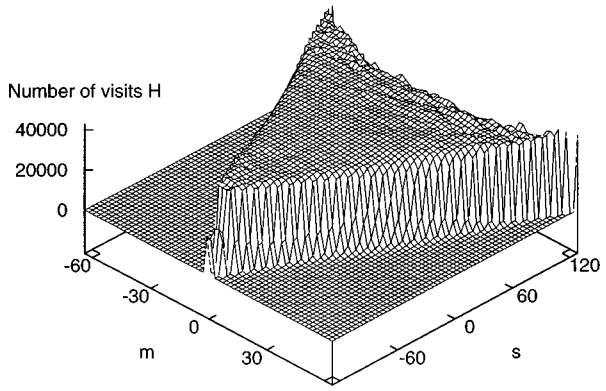

FIG. 3. Perspective view of the histogram $H_4(m,s)$ (the number of visits of the macrostate $\{m,s\}$) provided by the fourth Monte Carlo stage for the 8×8 lattice.

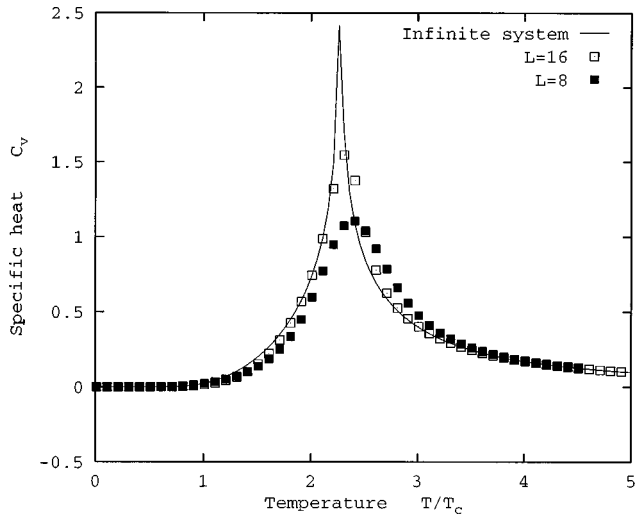

FIG. 4. Specific heat—fluctuations of energy per site with the energy in temperature units—computed by the present method for finite systems: 8×8, 16×16; full line: Onsager solution.

process, so that the standard deviation of τ is comparable to $\langle\tau\rangle$; thus the SD region was also called the ''stochastic'' region. In the MD region, $\langle\tau\rangle$ is quite short and independent of system size [35,36,20] while the standard deviation of τ is much smaller than $\langle\tau\rangle$ so that it was called the ''deterministic'' region. The DSP crossover depends on the system's size and temperature. For ''ultraweak'' fields (within the stochastic region) the critical droplet's size may be larger than the system size; the system is ''metastable'' as long as the whole system has not switched in the ''stable'' phase. In this case the system's behavior is similar to that at $h=0$ where two competing bulk phases coexist [12]. The corresponding crossover field was called the ''thermodynamical spinodal.'' (For a more detailed description on the subject see, e.g., Refs. [37,12,22].)

We have simulated, by Monte Carlo Metropolis dynamic, the relaxation paths projected in the (m,s) space, for the nearest-neighbor planar Ising systems already considered (sizes 8×8 and 24×24). It is worth showing one of these paths, plotted on the equilibrium distribution $P_\beta(m,s)$ surface. This is done in Fig. 5 and, from a simple glance, it can be conjectured that the Metropolis path, in the minor probability peak (i.e., near the metastable state) behaves stochastically; then, near and mainly after the saddle point, it behaves more or less deterministically, before ending, stochastically again, in the major probability peak, i.e., in the stable state.

A second major feature displayed by Fig. 5 is that the path seems to follow a line of high probability, i.e. a ridge of the probability surface. For a quantitative investigation of the problem, we have computed the following quantities.

(i) The mean metropolis (MM) path, obtained by averaging, for each m value, the s values given by typically 1000 independent Metropolis runs.

(ii) The equilibrium distribution (ED) path, conveniently obtained by a similar averaging of s values based on the equilibrium distribution

$$\overline{s_m}=\sum_s s.P_\beta(m,s)/P_\beta(m), \tag{9}$$

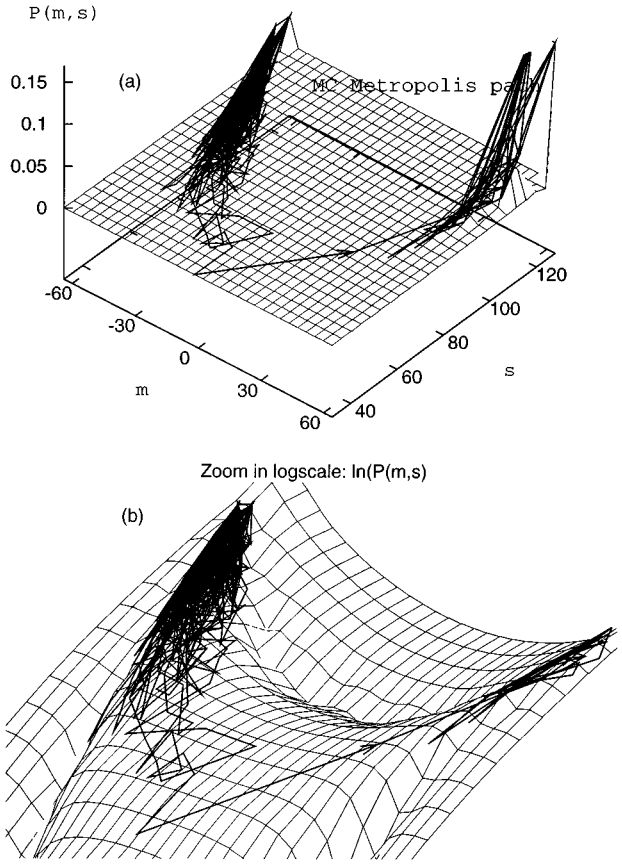

FIG. 5. The microscopic Metropolis relaxation path MM from the metastable phase (all spins down at positive field), projected over the two macroscopic variables s and m, is plotted over the probability surface $P_\beta(m,s)$ every 500 Monte Carlo steps per spin for the 8×8 system; $h/T=0.0125$ and $T=0.88Tc$. (a) Linear scale. (b) A zoom in semilogarithmic (ln) scale in order to display the details around the saddle point. Obviously, the system spends much more time around the probability peak over the metastable phase's macrostates than around the saddle-point area.

where $P(m,s)/P(m)$ is the conditional probability for the system to be in the $\{m,s\}$ point, with m being fixed before. This approximately gives the ridge line. Actually, we computed the ED and the ridge values, and checked that they were reasonably close to each other, except for small sizes $(L<8)$ or for paths really near the edge of the allowed space state (i.e., for low temperatures).

We show in Fig. 6 (model size $L=8$) how the ED path depends on temperature: the higher the temperature, the smaller the correlations when the system escapes from the metastable state. Simple calculations on Eq. (9) show that the ED path does not depend on the field value; only the position of the saddle point moves along the path, from large negative m values (large fields) to small m values (weak fields). This is shown in Fig. 7, which displays the values $P(m,\overline{s_m})$ on the ED path for different h values.

Then the comparison between MM and ED paths, shown in Figs. 8 and 9, can be interpreted, distinguishing three field regions with respect to the saddle-point position on the ED surface: (1) The fields for which the saddle point is near $m=0$, corresponding to *weak* fields in the stochastic region far from the DSP crossover. (2) Fields whose saddle point

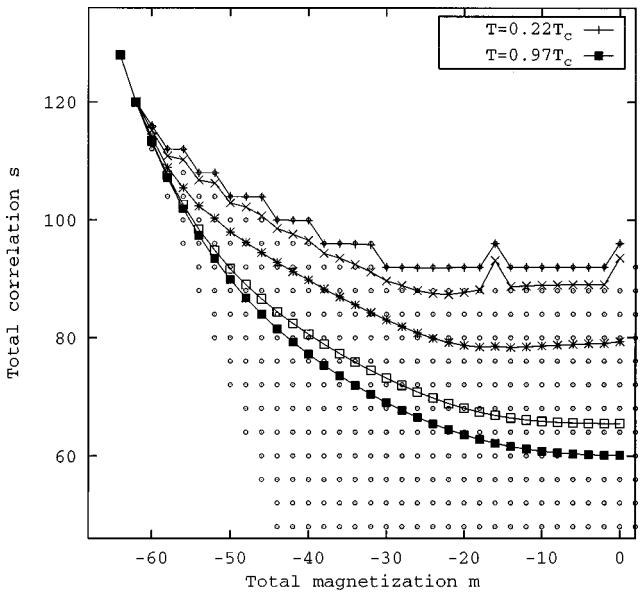

FIG. 6. Equilibrium distribution (ED) relaxation paths from the state $m=-N$ to $m=0$ plotted for five temperature values: $T/Tc=0.22$, 0.44, 0.66, 0.88, and 0.97 (from full squares to open circles); the ED paths do not depend on the field. The dots correspond to the $\{s,m\}$ states. At $T=0.22Tc$ the path passes by the edge of the space corresponding to the minimum of the interface between the two phases, i.e., the lower energy possible during the growing process; at this temperature there is only one droplet growing with the minimum of the interface—a circular droplet. When the temperature increases the system optimizes between low-energy macrostates and highly degenerated ones; i.e., the paths approach the highly degenerated center of the macrostate space.

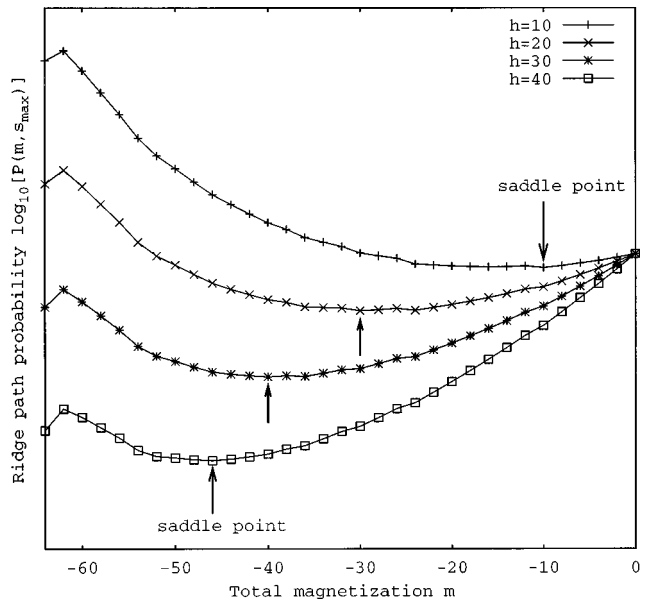

FIG. 7. The equilibrium probabilities of the $\{m,s\}$ points on the ED ridge path, plotted as a function of m, for four fields: $h/T=0.05$, 0.1, 0.15, and 0.2 (from crosses to open squares) at $T=0.88Tc$. The arrows at the minimum of these functions correspond to the saddle points: they move toward $m=-N$ as the field increases.

stays between $m=-N$ and $m=0$, corresponding to *intermediate* values laying in a large region around the DSP crossover. (3) Fields for which the saddle point vanishes on the ED surface which correspond to *strong* fields far behind the crossover in the deterministic region. We establish the DSP crossover field at the point where the standard deviation of the lifetime stays as half the lifetime as in Ref. [22]. The results are the following.

(i) *Weak and intermediate fields*. Starting from the metastable state, both paths closely coincide at the beginning and diverge very weakly (but progressively) when approaching the saddle point (Fig. 8), where relaxation becomes less stochastic (Fig. 5) However, before the saddle point (for these fields it is near $m=0$) the differences are small and decrease in reduced units (s divided by the total number of s values: $2N$) as the system's size increases. For these weak fields we can finally conclude that the escaping paths from the metastable phase can be deduced analytically from the ED surface. As the field increases a slight departure from the ED predictions toward lower correlation states (low-s values) starts closer to $m=-N$, and increases faster and faster; we observe that the progressive divergence between the two paths follows the displacement of the saddle point from $m=0$ to $m=-N$. In other words, a crossover from stochastic to deterministic relaxation is observed around the saddle-point position of the ED surface. It corresponds to the crossover from a metastable behavior to an unstable one.

(ii) *Strong fields.* The relaxation is deterministic all along; the paths strongly diverge on increasing fields (Fig. 9), the departure systematically directed toward lower correlation macrostates.

The above observations confirm that the ED description is still valid in metastable phase regions—i.e., weak fields or in

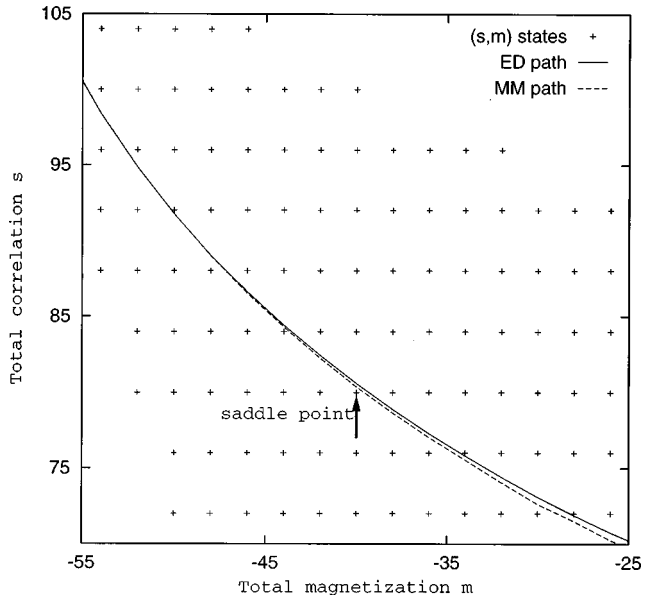

FIG. 8. Mean Metropolis (MM) relaxation path from $m=-N$ to $m=0$ at $T=0.88Tc$ and $h/T=0.15$ (dashed line) and the corresponding equilibrium distribution (ED) path (full line), plotted for the 8×8 system. The mean Metropolis path is calculated by averaging over 10^4 escapes from the metastable state. The arrow points out at the saddle point of the ED surface; the difference between the paths remains very small, but is already sizable before the saddle point. Note that this systematic regular departure toward high-density macrostates is in large excess of the various statistical scatters involved in the calculations.

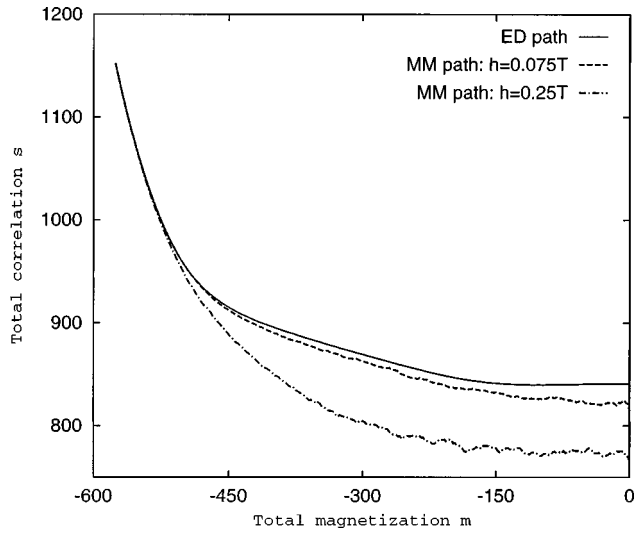

FIG. 9. Mean Metropolis (MM) paths for the 24×24 lattice plotted for relatively strong fields (with respect to the H_{DSP}): $h/T=0.075$ (dashed line) and $h/T=0.25$ (dot-dashed line) at $T=0.88Tc$. The full line shows the corresponding ED path; the ED surface has no saddle point at these fields.

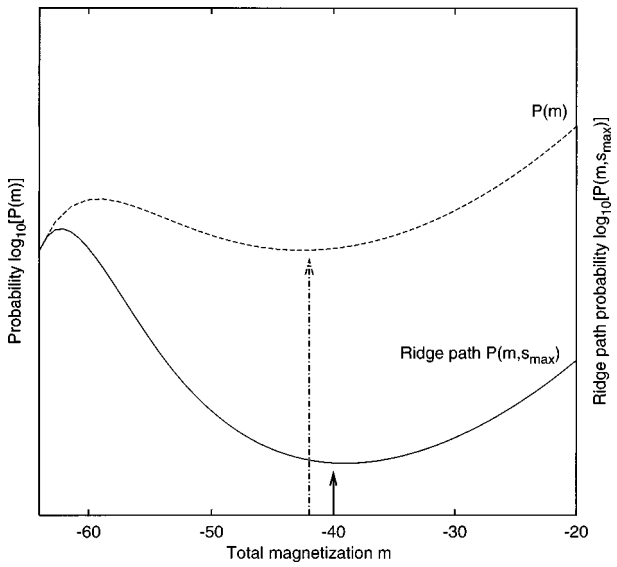

FIG. 10. The equilibrium distribution $P(m)$ (dashed line) and the equilibrium probabilities of the (s,m) points on the ED path (full line), plotted (both on a $\log_{10}$ scale) as a function of m for $h/T=0.25$, $T=0.88Tc$, for the 8×8 lattice. The minimum of $P(m)$ clearly differs from the minimum of $P(m,s_{\max})$ corresponding to the saddle point of the ED surface.

the beginning of the relaxation path for intermediate fields—while there is no clear-cut border for the metastable region in the macrostate space. In that sense, the conjecture mentioned in Sec. I about a Penrose-Lebovitz formalism of the metastable states even in systems with short-ranged interactions [10,15] is supported. It is worth noting that the accuracy of the ED description is highly related to the stochastic nature of the escape from the metastable phase. The stochastic nature is due to the presence of the energy barrier: the higher the barrier, the rarer the fluctuations leading to escape from the metastable phase. In such a case the system has much time, before it escapes, for exploring its configuration space [degeneracy $N(s,m)$ of the $\{s,m\}$ macroscopic states], obtaining ''knowledge'' of the macroscopic ED as in the equilibrium phase. The progressive crossover from stochastic to deterministic, i.e., from metastable to unstable regions of the macrostate space, is merely due to the progressive lowering of the free energy barrier. The departure of MM paths is systematically directed toward high-degenerated macrostates (the density's maximum is in the center of the macrostate space): when the barriers are low, it may be easier to escape passing by neighboring high-density states despite higher barriers.

It is clear that the ED description falls down for strong fields (h being of the same magnitude as J), where there are no more energy barriers for the single spin-flip: the system is prepared in an unambiguous unstable phase corresponding to a *purely out of equilibrium* feature, and leading to classical deterministic relaxation. In fact, if the energy decreases at each spin-flip proposal toward the stable phase, then all flips are accepted by the Metropolis dynamic and the behavior is purely deterministic. It is the case for fields larger than a crossover value $H_{\mathrm{uns}}=zJ$, with z the number of interacting neighbors. Then the system merely follows the higher density $N(m,s)$ path in the macrostate space, irrespectively of the field and temperature. The latter behavior (inherent to the absence of the energy barriers) is also observed in presence of weak energy barriers, i.e. for fields smaller than H_{uns}, as in Fig. 9 where are shown two MM paths for fields below and beyond H_{uns}. It is known [38] that dynamical properties far from equilibrium are highly dependent on the type of dynamic, e.g., the choice of the transition probabilities satisfying the detailed balance condition. It would be interesting to study other microscopic dynamics—Glauber, heat bath, or cluster dynamics like Wolff or Swendsen-Wang [24]—from the same viewpoint.

It is worth noting that the saddle point depends on the dimension chosen for the ED (hyper)surface. This is illustrated in Fig. 10, where the m value of a two-dimensional saddle-point position and the corresponding one-dimensional extremum value are compared. Consequently, the field value for which the saddle point vanishes (i.e., there are no longer free energy barriers beyond that field) depends on the dimension of the projected probability (free energy). Thus the system behavior is still stochastic even when the two-dimensionial probability surface no longer has a secondary peak: the latter should still exist in higher-dimensional ED spaces. Then another prospect would be obtaining higher-dimensional densities of states, e.g., including the number and (or) the size of the clusters, which are important in nucleation phenomena. Also, for a more quantitative evaluation of the ED description, a detailed study of the correlation beetween the two (or more) dimensional saddle points and the DSP introduced in Ref. [34] should be instructive.

IV. PERSPECTIVES AND DISCUSSION TOWARD A MULTIVARIABLE MACROSCOPIC DYNAMIC

Concerning the first slow part of the relaxation from the metastable state, the above macrostates being well described by the ED, it is appealing to substitute the Markovian microscopic local dynamic over the 2^N configurations by a macroscopic, still *Markovian* one over the $\sim N^2/2$ macrostates

$\{s,m\}$. In other words, when the system has sufficient time to explore all the configuration space associated with the macrostates defined here, it can be assumed that the detailed balance condition is also satisfied by the macrostates $\{s,m\}$. The fact that the last arguments are much less valid for the last and fast part of the relaxation is not of importance for the mean metastable lifetime, which is dominated by the slow part of the relaxation. This projection from a microscopic to macroscopic dynamic was previously proposed and checked in Ref. [22] for only one variable, the order parameter m. It was just mentioned there that such a macroscopic dynamic is an exact one only for long-ranged interaction equivalent-neighbor models [39], which are also called mean-field models. For short-ranged interaction systems this is only an approximation; the exact projection of the microscopic Markovian dynamic over macroscopic variables has no reason for being still Markovian. The reason is that, for the latter systems, the macrostates defined by the order parameter m contain nonequivalent microscopic configurations—they are equivalent only in the equivalent neighbor model—and the latter assumption leads to neglecting memory effect propagation from the *different* microscopic configurations corresponding to the same value of m. Hence, there it was called a mean-field dynamic. As was argued in that work [22], the macroscopic dynamic for short-ranged interactions may be a good approximation for slow variables such as m and E in the metastable state (see also Refs. [40,41]). Obviously, a macroscopic dynamic over the variables m and s, being equivalent to m and E (Sec. II A), stands no less as an approximation of the underlying microscopic dynamic than the one-variable macroscopic dynamic of Ref. [22]: different microscopic configurations belonging to the same macrostate may lead to very different features for the future. However, there is much less information neglected by the macrostates $\{s,m\}$ than by those defined only by m, the more so because we also define the macrostates by the energy. Nevertheless, the supplementary information from the microscopic droplet picture, coming from the variable s, is no more than the total length of the interface between up- and down-spin areas.

The complete knowledge of the macrostate probabilities enables establishing the balance condition

$$P(\{s,m\}_k)W(k,k')=P(\{s,m\}_{k'})W(k',k) \qquad (10)$$

corresponding to a Markovian dynamic. The interest of the latter lies in the fact that it leads to very simple calculations: in principle, calculating all the moments of the metastable lifetime distribution can be reduced to the inversion of the **W** matrix [42,22], satisfying Eq. (10) (the latter is an $M\times M$ matrix, where M is the number of states). While the corresponding matrix of the microscopic dynamics is an $2^N x 2^N$ matrix—and then one can only do Monte Carlo simulations—the matrix inversion is possible for the present macroscopic dynamic for which the number of macrostates $\{s,m\}$ is $\sim N^2/2$. Then the lifetime calculation, which no longer involves a simulation (equivalent to an integration over time), is independent of the lifetime value.

In order to keep the same local dynamic, the permitted transitions between macrostates are restricted to single spin flips, i.e., m values differ by ± 2 and s values differ by $\pm 8 \pm 4$ or 0. There is not a unique transition matrix **W** satisfying Eq. (10) (i.e., there is not only one stochastic dynamic leading to equilibrium); we choose simple Metropolis-type matrix elements

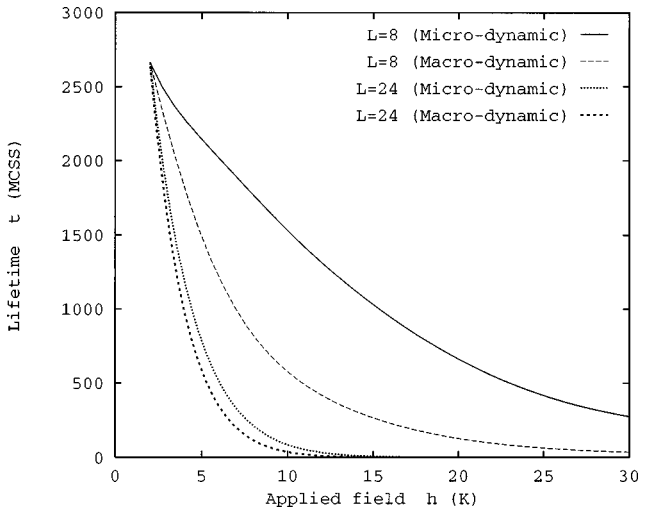

FIG. 11. The average lifetime of the metastable state (relaxation time from $m=-N$ to $m=0$) obtained by Monte Carlo simulations with the microscopic Metropolis dynamic and with the macroscopic Metropolis dynamic, plotted as a function of the applied field, for the 8×8 lattice (upper curves) and the 24×24 lattice (lower curves) both at $T=0.88Tc$. The field varies in the stochastic region. All values are calculated by averaging over 1000 independent paths. The time scales (in units of Monte Carlo steps per site MCSS are adapted to fit each other at the lower field value. The field is in energy, i.e., temperature, units.

$$W(\{m,s\},\{m',s'\})=\min\left\{1,\frac{P(m',s')}{P(m,s)}\right\}, \qquad (11a)$$

with $m'=m\pm 2$ and $s'=s\pm k$, where $k=0,\pm 4,\pm 8$,

$$W(\{m,s\},\{m,s\})=1-\sum_{\{m',s'\}\neq\{m,s\}} W(\{m,s\},\{m',s'\}). \qquad (11b)$$

Solving the macroscopic dynamic by the Monte Carlo method, we obtained both lifetimes and relaxation paths, leading to the following observations.

(i) The microscopic and macroscopic dynamics paths similarly compare to the two-dimensional ED path, although the macroscopic dynamics depends only on the two variables s and m of the above equilibrium distribution. This means that the progressive departure from the ED description is really inherent to the metastable character of the initial state; that is, to the escape from the quasistationary stationary situation corresponding to the metastable phase toward the nonstationary, out-of-equilibrium situation.

(ii) The comparison between the relaxation paths from the microscopic and macroscopic dynamics confirms both assumptions of phenomenological macroscopic kinetic theories [43,31–33] (for a review, see, e.g., Refs. [44–46] and the results of previous work which compare between different microscopic dynamics [20] and between microscopic and one-variable macroscopic dynamics [22]. That is, when the

macroscopic relaxation is very slow with respect to the time scale of the dynamic details (as it is for the first and long part of the relaxation path), the process is weakly dependent on the type of dynamic. Indeed, in phenomenological theories it is assumed that in this case the details of the dynamics are averaged, and the behavior of the system is only governed by free-energy changes [44]. In addition, we show that the first long part of the decay nearly fits the equilibrium distribution.

(iii) In a second step we have investigated the lifetimes: the computed mean lifetime values, given by the microdynamics and macrodynamics, as a function of the applied field, are reported in Fig. 11. The microdynamics and macrodynamics compare well for the larger size, where the ED surface is steep around the ridge path. In this case, due to the presence of high-energy barriers, the scatter of microscopic relaxation paths, during the first and long part of the decay, is relatively weak, as is suggested by the projection over the two macroscopic parameters m and s showed in Fig. 5 (or by the comparison between the standard deviations on the s_m values for the two sizes: 8×8 and 24×24). Therefore, the details of hidden microscopic paths are not able to modify the future sizably: memory effect propagation through variables other than s and m is not efficient, and the Markovian macroscopic dynamics is a very good approximation.

In summary, we studied the relations between the features of the two-dimensional macroscopic ED and the relaxation from a metastable state. The projected relaxation paths are directly obtained by a projected ED, with excellent accuracy, and the associated stochastic macroscopic dynamics is a good approximation of the exact projection of the microscopic one. Of course, the ED description fails when the system relaxes from an unstable state. These results are highly encouraging for investigating metastable states via an analytical-like method, which is free from the unavoidable limitations of the microscopic (time integrationlike) Monte Carlo simulations. The determination of relaxation paths may be very useful for systems with more than one metastable phase (the Blume-Capel model for a three-state system) so as to predict the probabilities for visiting the states with different orderings.

ACKNOWLEDGMENTS

The authors would like to thank Dr. V. Pontikis, Dr. A. Finel, Dr. H. Spiering, and Dr. K. Boukhedaden for very stimulating discussions, and Dr. J. Hodges for a critical reading of the manuscript. Acknowledgments are due to the Calculus and Research Center of the University of Paris for the IBM RS/6000 computer time. Laboratoire de Magnétisme et d'Optique is supported by CNRS, as Unité de Recherche Associée No. 1531. I. Shteto would like to thank the Entraide Universitaire Française Foundation for financial support.

[1] P. Gütlich, A. Hauser, and H. Spiering, Angew. Chem. Int. Ed. Engl. **33**, 2024 (1994).
[2] A. Bousseksou, J. Nasser, J. Linares, K. Boukheddaden, and F. Varret, J. Phys. (France) I **2**, 1381 (1992).
[3] K. Boukheddaden, J. Linares, and F. Varret, Phys. Rev. B **47**, 14 070 (1993).
[4] K. Boukheddaden, J. Linares, and F. Varret, Phys. Rev. B **49**, 15 664 (1994).
[5] K. Boukheddaden and F. Varret, Phys. Rev. B **53**, 1 (1996).
[6] G. L. Sewell, Ann. Phys. (N.Y.) **97**, 55 (1976).
[7] G. L. Sewell, Commun. Math. Phys. **55**, 63 (1977).
[8] G. L. Sewell, Phys. Rep. **57**, 307 (1980).
[9] G. L. Sewell, in *Quantum Theory of Collective Phenomena* (Clarendon, Oxford, 1989), Chap. 6, pp. 169–171 and 183–188.
[10] D. Capocaccia, M. Cassandro, and E. Olivieri, Commun. Math. Phys. **39**, 185 (1974).
[11] P. Vanheuverzwijn, J. Math. Phys. **20**, 2665 (1979).
[12] P. A. Rikvold, H. Tomita, S. Miyashita, and S. W. Sides, Phys. Rev. E **49**, 5080 (1994).
[13] M. A. Novotny, Phys. Rev. Lett. **74**, 1 (1995).
[14] O. Penrose and J. L. Lebowitz, J. Stat. Phys. **3**, 211 (1971).
[15] O. Penrose and J. L. Lebowitz in *Fluctuation Phenomena*, edited by E. W. Montroll and J. L. Lebowitz (North-Holland, Amsterdam, 1987), Chap. 5.
[16] L. S. Schulman, J. Phys. A **13**, 237 (1980).
[17] K. Binder and M. H. Kalos, J. Stat. Phys. **22**, 363 (1980).
[18] H. Furukawa and K. Binder, Phys. Rev. B **26**, 556 (1982).
[19] K. Kaski, K. Binder, and J. D. Gunton, Phys. Rev. B **29**, 3996 (1984).
[20] T. S. Ray and P. Tamayo, J. Stat. Phys. **60**, 851 (1990).
[21] T. S. Ray and J. S. Wang, Physica A **167**, 580 (1990).
[22] J. Lee, M. A. Novotny, and P. A. Rikvold Phys. Rev. E **52**, 356 (1995).
[23] J. Lee, Phys. Rev. Lett. **71**, 211 (1993); **71**, 2353(E) (1993).
[24] R. H. Swendsen, J. S. Wang, and A. M. Ferrenberg, in *Monte Carlo Methods in Condensed Matter Physics*, edited by K. Binder (Springer-Verlag, Berlin, 1992).
[25] A. M. Ferrenberg and R. H. Swendsen, Phys. Rev. Lett. **63**, 1195 (1989).
[26] J. P. Valleau and D. N. Card, J. Chem. Phys. **57**, 5457 (1972).
[27] C. H. Bennett, J. Comput. Phys. **22**, 245 (1976).
[28] A. M. Ferrenberg and R. H. Swendsen, Phys. Rev. Lett. **61**, 2635 (1988).
[29] B. A. Berg and T. Neuhaus, Phys. Rev. Lett. **68**, 9 (1992).
[30] J. Lee, Phys. Rev. Lett. **71**, 2353(E) (1993).
[31] J. S. Langer, Ann. Phys. (N.Y.) **41**, 108 (1967).
[32] J. S. Langer, Phys. Rev. Lett. **21**, 973 (1968).
[33] J. S. Langer, Ann. Phys. (N.Y.) **54**, 258 (1969).
[34] H. Tomita and S. Miyashita, Phys. Rev. B **46**, 8886 (1992).
[35] E. P. Stoll and T. Schneider, Physica B & C **86–88**, 1419 (1977).
[36] D. Stauffer, Int. J. Mod. Phys. C **3**, 1059 (1992).
[37] P. A. Rikvold and B. M. Gorman, in *Annual Reviews of Computational Physics I*, edited by D. Stauffer (World Scientific, Singapore, 1994).
[38] H. Müller-Krumbhaar and K. Binder, J. Stat. Phys. **8**, 1 (1973).
[39] R. B. Grifiths, C.-Y. Weng, and J. S. Langer, Phys. Rev. **149**, 301 (1966).
[40] H. Grabert, Z. Phys. B **26**, 79 (1977).

[41] H. Grabert, *Projection Operator Techniques in Nonequilibrium Statistical Mechanics* (Springer, Berlin, 1982).

[42] M. Iosifescu, *Finite Markov Processes and Their Applications* (Wiley, New York, 1980), p. 99.

[43] R. Becker and W. Döring, Ann. Phys. (Leipzig) **24**, 719 (1935).

[44] H. Metiu, K. Kitahara, and J. Ross, in *Fluctuation Phenomena*, edited by E. W. Montroll and J. L. Lebowitz (North-Holland, Amsterdam, 1987), Chap. 4.

[45] J. D. Gunton and M. Droz, in *Introduction to the Theory of Metastable and Unstable States*, Lecture Notes in Physics Vol. 183 (Springer, Berlin, 1983).

[46] J. D. Gunton, M. San Miguel, and P. S. Sahni, in *Phase Transition and Critical Phenomena 8*, edited by C. Domb and J. L. Lebowitz (Academic, London, 1983), Chap. 3.